

C. elegans PAT-4/ILK Functions as an Adaptor Protein within Integrin Adhesion Complexes

A. Craig Mackinnon,¹ Hiroshi Qadota,²
Kenneth R. Norman,² Donald G. Moerman,²
and Benjamin D. Williams^{1,3}

¹Department of Cell and Structural Biology
University of Illinois, Urbana-Champaign
601 South Goodwin Avenue
Urbana, Illinois 61801

²Department of Zoology
University of British Columbia
Vancouver, British Columbia V6T 1Z4
Canada

Summary

Background: Mammalian integrin-linked kinase (ILK) was identified in a yeast two-hybrid screen for proteins binding the integrin β_1 subunit cytoplasmic domain. ILK has been implicated in integrin-mediated signaling and is also an adaptor within integrin-associated cytoskeletal complexes.

Results: We identified the *C. elegans pat-4* gene in previous genetic screens for mutants unable to assemble integrin-mediated muscle cell attachments. Here, we report that *pat-4* encodes the sole *C. elegans* homolog of ILK. In *pat-4* null mutants, embryonic muscle cells form integrin foci, but the subsequent recruitment of vinculin and UNC-89 as well as actin and myosin filaments to these *in vivo* focal adhesion analogs is blocked. Conversely, PAT-4/ILK requires the ECM component UNC-52/perlecan, the transmembrane protein integrin, and the novel cytoplasmic attachment protein UNC-112 to be properly recruited to nascent attachments. Transgenically expressed “kinase-dead” ILK fully rescues *pat-4* loss-of-function mutants. We also identify UNC-112 as a new binding partner for ILK.

Conclusions: Our data strengthens the emerging view that ILK functions primarily as an adaptor protein within integrin adhesion complexes and identifies UNC-112 as a new ILK binding partner.

Introduction

Caenorhabditis elegans has proven to be an advantageous system for the genetic analysis of muscle development [1, 2]. Myoblasts are born near the end of gastrulation and soon begin to express muscle-specific structural proteins [3, 4]. Subsequently, they migrate to their final positions in the body wall and flatten against the hypodermis, or “skin” of the embryo [5, 6]. Structural proteins, such as integrin and vinculin, then polarize and accumulate at the basal sarcolemma adjacent to the hypodermis where they assemble into a highly ordered set of related muscle attachment structures [4] called dense bodies and M-lines, which attach actin thin filaments and myosin thick filaments, respectively, to the basal sarcolemma (Figure 1). Based upon their function

and polypeptide composition [7–14], dense bodies and M-lines are analogs and indeed homologs of vertebrate adhesion plaques (Figure 1C).

We are focusing upon a subset of *C. elegans* Pat mutants (Paralyzed, Arrested elongation at Two-fold) [15] that have deficits in dense body and M-line assembly. The corresponding genes investigated to date include *unc-52* [7], *pat-3* [8], *unc-112* [11], *unc-97* [10], and *deb-1* [13, 16], each encoding a muscle attachment protein (Figure 1C). Here, we report our investigation of *pat-4*, which we show codes for the nematode homolog of integrin-linked kinase (ILK), a vertebrate focal adhesion protein implicated in integrin signaling [17, 18].

ILK was first identified in a yeast two-hybrid screen using the integrin β_1 subunit cytoplasmic domain as bait [19]. ILK has four N-terminal ankyrin repeats, followed by a pleckstrin homology domain that partially overlaps a C-terminal kinase domain [20]. The ankyrin repeats bind to the first LIM domain of UNC-97/PINCH [10, 21], a LIM-only focal adhesion adaptor protein, while the pleckstrin homology domain has been proposed to bind phosphoinositides, which can activate the kinase activity of ILK *in vitro* [20]. The ILK kinase domain, which is most similar to the serine/threonine kinase Raf, binds the integrin β_1 subunit cytoplasmic tail [19]. Functional analysis of ILK has relied heavily upon the expression of high levels of wild-type and “kinase-dead” forms of the protein in cultured cells. A wide range of effects has been reported in these experiments, and significant attention has focused upon the Wnt signaling pathway [20, 22] and alterations in the protein kinase B (PKB/AKT) pathway regulating apoptosis [20]. It is of particular interest, therefore, that a recently reported reverse genetic analysis of ILK function in *Drosophila* failed to find evidence for ILK function in well-characterized PKB or Wnt signaling pathways [23]. In fact, these authors showed that a kinase-dead ILK construct rescues ILK mutants as well as the wild-type gene. They did find that ILK colocalizes with integrin and is needed to stabilize muscle attachments, leading them to propose that ILK functions primarily as an adaptor molecule.

Here, we show that PAT-4/ILK is a component of *C. elegans* muscle dense bodies and M-lines and is needed for their proper assembly. In reciprocal investigations, we show that PAT-4/ILK is dependent upon integrin for its assembly into muscle attachments. Kinase-dead forms of PAT-4/ILK rescue the mutant *pat-4* phenotype, and we also have failed to find any evidence for PAT-4/ILK function in Wnt signaling cascades. Our results therefore concur with the findings from the *Drosophila* ILK analysis, suggesting that ILK functions primarily as an adaptor molecule during muscle assembly. We extend these results by identifying the ERM adhesion complex protein UNC-112 [11] as a new ILK-interacting partner.

Results

pat-4 Encodes Integrin-Linked Kinase

We used a combination of positional cloning and candidate gene approaches to molecularly isolate the *pat-4*

³Correspondence: bdwillms@uiuc.edu

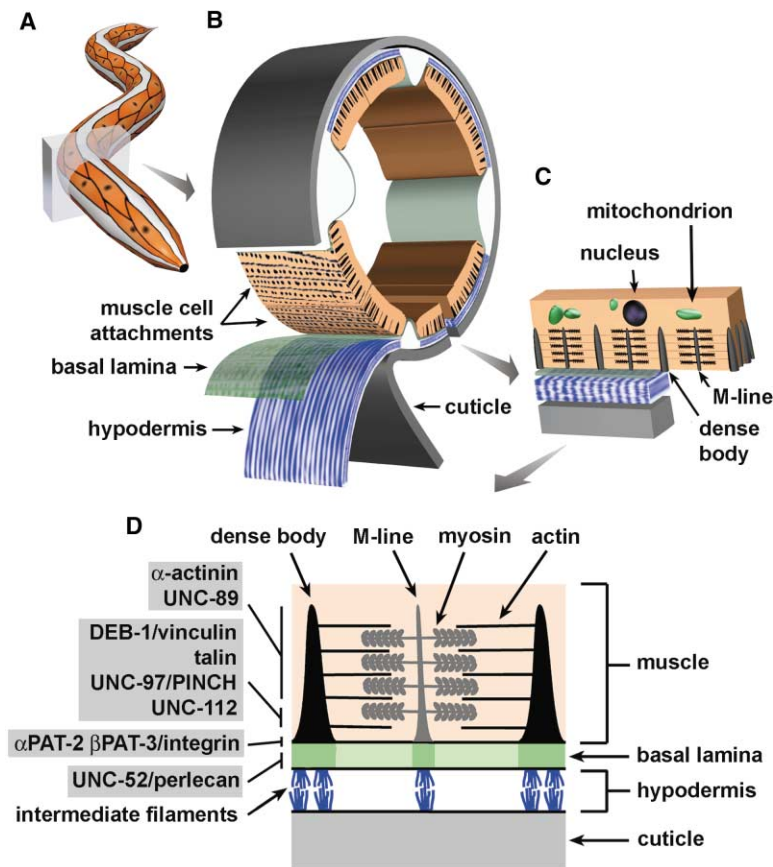


Figure 1. Schematic Diagram of the *C. elegans* Body-Wall Muscle Structure

(A) An adult worm with body-wall muscle quadrants visible (orange).

(B) A body-wall cross-section with cuticle, hypodermis, and basal lamina peeled away to reveal the basal membrane of two body-wall muscle cells.

(C) A longitudinal section through a body-wall muscle cell. Dense bodies and M-lines attach actin thin filaments and myosin thick filaments, respectively, to the basal sarcolemma.

(D) Locations of several different muscle attachment proteins. α -actinin and vinculin are present in dense bodies but not M-lines. Conversely, UNC-89 is present only in M-lines. Localization of the α PAT-2 integrin subunit is unpublished data from B.D.W. and R. Waterston.

gene (Figure 2A). RNA interference (RNAi) experiments performed on predicted gene C29F9.7 produced 98% Pat F1 progeny ($n > 4000$). Subsequent transformation experiments confirmed that a genomic DNA fragment containing C29F9.7 completely rescues the phenotype of *pat-4* homozygotes. Two of the four existing *pat-4*

alleles are point mutations (Figure 2C) in C29F9.7, including a nonsense mutation within the N-terminal part of the protein-coding region, providing unambiguous confirmation of the *pat-4* molecular identity. The remaining two *pat-4* alleles are deletions that completely remove C29F9.7 (see the Experimental Procedures). Embryos homozygous for the nonsense allele *pat-4(st551)* fail to stain with PAT-4 polyclonal antiserum and are therefore likely to be protein null. The predicted primary peptide structure of PAT-4 is similar (56% identity) to the human molecule integrin-linked kinase (ILK) (Figure 2D). Searches of the essentially complete *C. elegans* genome sequence show that PAT-4 is the sole *C. elegans* ILK homolog. We refer to the PAT-4 protein as PAT-4/ILK.

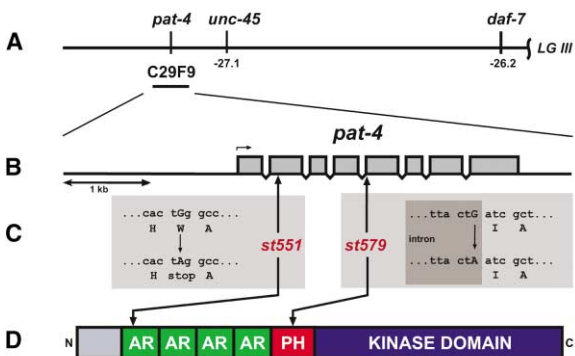


Figure 2. Molecular Isolation of *pat-4*

(A) A genetic map of the left arm of *LG III*. The genomic cosmid clone C29F9 rescues *pat-4* mutant embryos.

(B) A genomic structure of the *pat-4* gene. Exons (gray boxes) and the methionine start codon (small arrow) are indicated.

(C) *pat-4* point mutations *st551* and *st579*.

(D) A structure of the predicted PAT-4/ILK protein. This diagram has been simplified. The C-terminal half of the PH motif is actually contained within the kinase domain.

PAT-4/ILK Colocalizes with Integrin

Transgenic minigenes encoding translational fusions between PAT-4/ILK and either green or yellow fluorescent protein (GFP, YFP) fully rescue *pat-4(st551)* mutants, providing strong evidence that the fusion proteins are functional *in vivo* and are likely to have a functionally relevant subcellular localization. Immunostaining experiments using anti-PAT-4/ILK show an identical localization pattern in wild-type embryos and adults (see below, and data not shown).

The *pat-4::gfp* transgene is initially expressed weakly throughout postgastrulation embryos (data not shown). By 420 min postfertilization, PAT-4/ILK::GFP is primarily

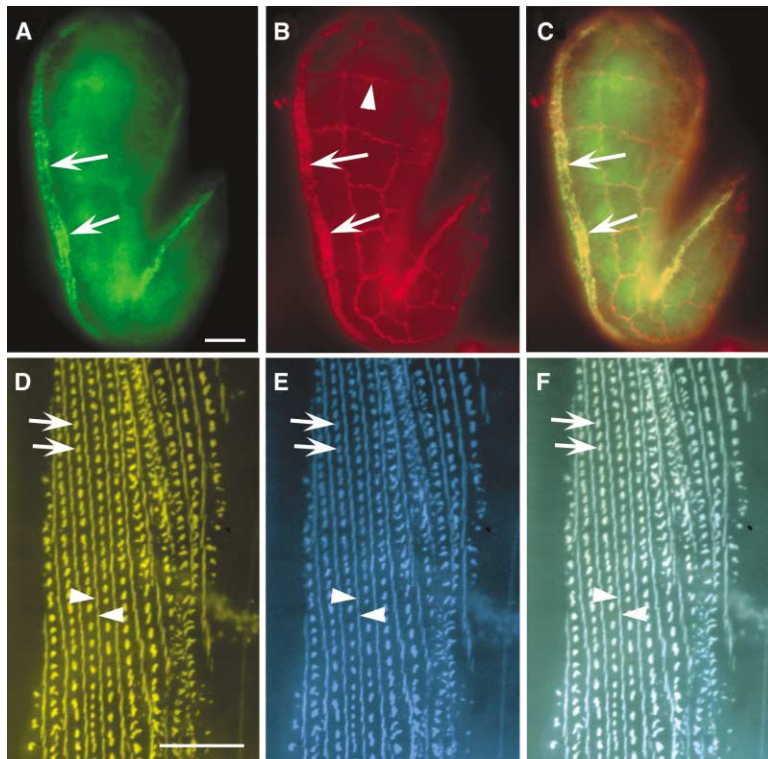


Figure 3. PAT-4/ILK and β PAT-3 Integrin Colocalize at Muscle Attachments

(A) A wild-type, \sim 420 min embryo. PAT-4::GFP localizes to body-wall muscle attachments (arrow). The scale bar represents 2 μ m. (B) The same embryo as that shown in (A) double stained with monoclonal antibodies MH25, recognizing β PAT-3 integrin, and MH27, recognizing hypodermal-hypodermal cell junctions (included for developmental staging and orientation purposes).

(C) An overlay of (A) and (B). Areas of PAT-4::GFP and integrin colocalization appear yellow.

(D–F) Detail of body-wall muscle from a rescued *pat-4(st551)* adult hermaphrodite coexpressing (D) *pat-4::yfp* and (E) *pat-3::cfp*. Dense body (arrows) and M-line (arrowheads) attachment structures are indicated. (F) An overlay of panels (D) and (E). Regions in which β PAT-3::CFP and PAT-4::YFP colocalize appear white. The scale bar in (D) represents 5 μ m.

observed in the body-wall muscle cells (Figure 3A), where it colocalizes with the integrin β PAT-3 subunit (Figures 3A–3C). *pat-4::gfp* is also transiently expressed in the pharynx during embryogenesis (data not shown). In adult hermaphrodites, *pat-4::gfp* expression is observed in body-wall muscle cells (Figure 3D), the spermatheca, the vulva muscles, a subset of the mechanosensory neurons (ALM, AVM, PLM, and PVM), the distal tip cells, the uterine muscles, and the anal depressor and anal sphincter muscles (data not shown). In adult body-wall muscle cells, PAT-4/ILK::YFP colocalizes with a functional β PAT-3::CFP integrin subunit in M-lines and dense bodies (Figures 3D–3F) and at muscle-muscle adherent junctions (data not shown). PAT-4/ILK::GFP is located near the cell membrane and does not extend very deeply into body-wall muscle cells. An identical localization has been reported previously for UNC-97/PINCH [10] and UNC-112 [11]. The fact that PAT-4/ILK is only observed at sites reported to contain the β PAT-3 integrin subunit in body-wall muscle cells (see below) is an expected result based on the studies of mammalian and *Drosophila* ILK [23, 24].

PAT-4/ILK Is Required for Dense Body and M-Line Assembly

Previous analysis of actin and myosin organization in the embryonic muscles of *pat-4* mutants revealed defects in sarcomere assembly quite similar to those in *unc-52* perlecan and *pat-3* integrin loss-of-function mutants [15]. In both *unc-52* and *pat-3* mutants, structural proteins do not polarize to the muscle cell basal membrane, and integrin fails to aggregate into nascent attachments [4, 15]. To determine the extent of dense body and M-line assembly in *pat-4* embryos, we investigated the localiza-

tion of UNC-52/perlecan and β PAT-3 integrin by antibody staining. The early localization of UNC-52/perlecan into a longitudinal stripe adjacent to each muscle occurs normally in *pat-4* mutants (compare arrows in Figures 4A and 4B). The initial polarization and subsequent clustering of integrin into foci also occurs normally (compare arrows in Figures 4C and 4D). There is, however, some irregularity in the integrin pattern in the *pat-4* mutant embryos. Some of the integrin foci are not located within the tight stripe of nascent attachments that normally forms near the centerline of each quadrant. Instead, they are in positions that are spread out laterally across the entire width of each muscle cell (arrowheads, Figure 4C). Integrin organization never improves in the *pat-4* embryos and, in fact, deteriorates in older animals (data not shown). In contrast, in wild-type embryos, the integrin foci soon organize further, forming a highly ordered striated array of morphologically distinguishable dense bodies and M-lines [4].

Formation of integrin foci in *pat-4* mutants suggests that dense body and M-line assembly is initiated in the absence of PAT-4/ILK protein. We next asked whether several dense body- and M-line-specific proteins are recruited to the integrin foci. In wild-type embryos 430 min postfertilization, the dense body protein DEB-1/vinculin has already polarized to the basal sarcolemma and is organized into nascent attachments that appear as a continuous stripe of staining along each muscle quadrant (Figure 4E). By 520 min, this pattern resolves into a recognizable array of dense bodies (see Figure 6C in [4]). In contrast, DEB-1/vinculin polarizes within the *pat-4* embryos but does not appear to fully assemble into nascent attachments (Figure 4F), as indicated by the different integrin and DEB-1/vinculin localization in

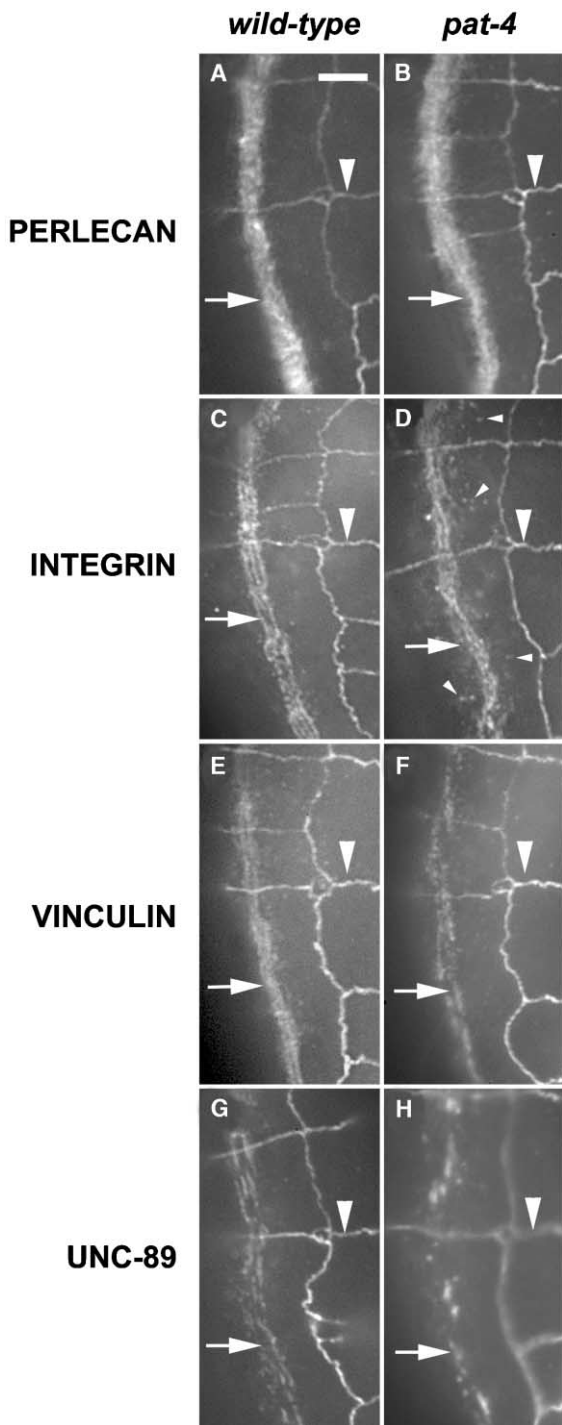


Figure 4. Muscle Assembly in *pat-4* Mutant Embryos
(A–H) Wild-type (left column) and *pat-4(st551)* mutant (right column) embryos 430 min postfertilization stained for (A and B) perlecan (antibody MH2), (C and D) integrin (antibody MH25), (E and F) vinculin (antibody MH24), and (G and H) UNC-89 (antibody MH42). All animals were also stained with antibody MH27 to show hypodermis-hypodermis junctions (arrowhead, all panels). The circular hypodermal cell junction formed at the derid sensillum is seen in all panels and can be used for orientation. All panels show a dorsolateral view of the embryo. One of the two dorsal body-wall muscle quadrants (arrow in all panels) is in the plane of focus. We obtained identical results for all four *pat-4* mutants. The scale bar in (A) represents 2 μ m.

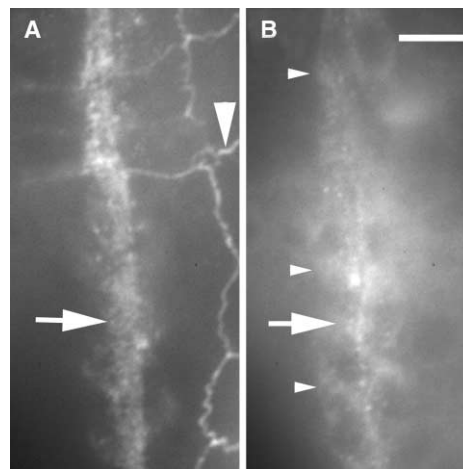


Figure 5. Integrin and UNC-112 Do Not Colocalize Extensively in a *pat-4(st551)* Mutant

(A) At \sim 430 min postfertilization, β PAT-3 integrin, stained with antibody MH25, is located in nascent muscle attachments. (B) A GFP channel in the same focal plane as (A). UNC-112::GFP is observed in some foci (arrows), but, for the most part, does not colocalize with integrin and instead is distributed diffusely within the cytoplasm (small arrowheads).

pat-4 mutants (compare arrows in Figures 4D and 4F). We also investigated the M-line protein UNC-89, which, in wild-type embryos, becomes polarized and recruited into an array of nascent M-lines [4]. In *pat-4* mutants, UNC-89 fails to polarize and remains in a large clump within the cytoplasm of each muscle cell (compare arrows in Figures 4G and 4H), indicating that UNC-89 also fails to be recruited to the nascent M-lines formed in the absence of PAT-4/ILK.

Because our previous work has shown that UNC-112 and integrin colocalize at muscle attachment structures [11], we were interested in determining if this colocalization requires PAT-4/ILK. Our efforts to generate antisera directed against UNC-112 were unsuccessful. Therefore, to determine the localization of UNC-112 in *pat-4(st551)* mutant embryos, we first crossed an *unc-112::gfp* transgene [11] into *pat-4* mutants and then stained the mutant embryos with β PAT-3 integrin antisera. In *pat-4* mutants, we observe that UNC-112 does not appear to extensively colocalize with integrin in the sarcolemmas (compare Figures 5A and 5B). Instead, UNC-112 mainly appears to be distributed diffusely throughout the cytoplasm (arrowheads, Figure 4B), suggesting that PAT-4/ILK is required for UNC-112 to properly assemble into nascent attachments. Identically staged wild-type embryos expressing the same *unc-112::gfp* transgene and stained with the same β PAT-3 monoclonal antibody show extensive colocalization of UNC-112 and β PAT-3 (see Figures 5G–5F from [11]).

Perlecan, Integrin, and UNC-112, but Not Vinculin, Are Necessary for PAT-4/ILK Assembly

In order to determine the requirements for PAT-4/ILK recruitment to muscle attachments, we generated an antibody to PAT-4/ILK and used it to localize this protein in wild-type embryos and in mutants blocked at different

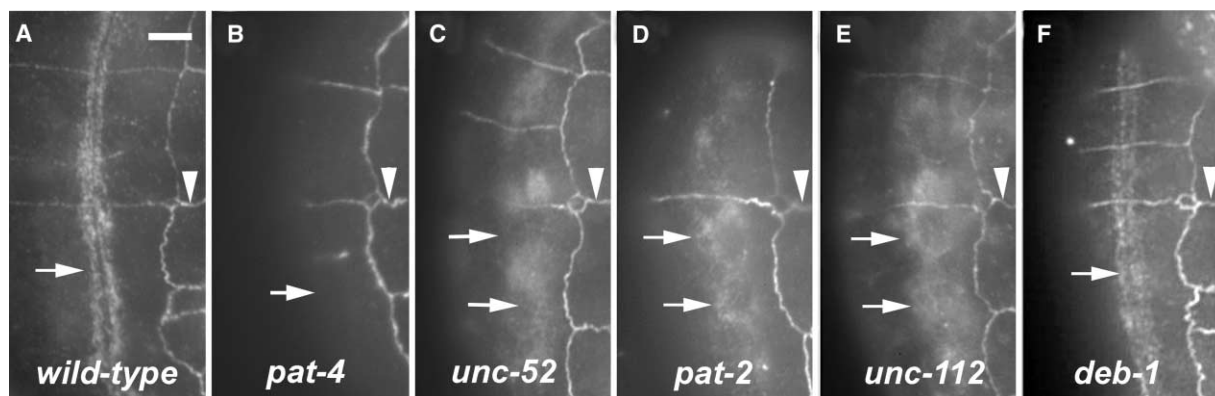


Figure 6. PAT-4/ILK Assembly at the Muscle Cell Membrane Is Blocked in *unc-52* Perlecan, *pat-2* Integrin, and *unc-112* Mutants, but Not in *deb-1* Vinculin Mutants

(A–F) Same view and developmental stage as in Figure 3. Embryos were double stained with anti-PAT-4 and with antibody MH27 to show hypodermal junctions (arrowheads). See Results for details. The scale bar in (A) represents 2 μ m.

stages of attachment assembly. This antiserum is specific to PAT-4/ILK, indicated by failure to detect any PAT-4/ILK protein in *pat-4(st551)* mutants (Figure 6B). This figure shows a *pat-4(st551)* embryo double stained with anti-PAT-4/ILK and antibody MH27, the latter of which stains hypodermal-hypodermal junctions and is included for orientation purposes. Body-wall muscle cells do not stain (arrow, Figure 6B), and only the MH27 staining pattern is observed (arrowhead, Figure 6B). In wild-type embryos, PAT-4/ILK polarizes and is recruited to nascent muscle attachments (Figure 6A). It has been shown previously that, in protein null *unc-52* perlecan mutants, integrin and other structural proteins including vinculin fail to polarize, and muscle attachments do not form [7, 15]. We stained *unc-52* perlecan mutants with the anti-PAT-4/ILK antiserum and found that PAT-4/ILK also fails to polarize to the membrane, accumulating instead in the cytoplasm (Figure 6C, compare with wild-type in Figure 6A). *pat-2* codes for the α PAT-2 integrin subunit in dense bodies and M-lines (unpublished data), and *pat-3* codes for the β PAT-3 integrin subunit [8]. It has been shown previously that muscle structural proteins fail to polarize in *pat-3* integrin mutants, accumulating instead in the muscle cell cytoplasm [4]. We stained both *pat-2* integrin α subunit (Figure 6D) and *pat-3* integrin β subunit mutant embryos (data not shown) and found that much of the PAT-4/ILK staining is distributed throughout the muscle cell cytoplasm (Figure 6D, arrow). PAT-4/ILK has a similar mislocalization in *unc-112* mutants (Figure 6E, arrow). It has also been shown that, in *deb-1* vinculin protein null mutants, integrin forms recognizable arrays of dense bodies and M-lines, but the recruitment of actin filaments to the sarcolemma fails to occur, indicating that dense body assembly is incomplete [4, 16]. We find that PAT-4/ILK is able to polarize and localize into nascent attachments in *deb-1* vinculin mutants (arrow, Figure 6F), indicating that vinculin is not required to recruit PAT-4/ILK to dense bodies.

PAT-4/ILK Binds UNC-112 in Yeast Two-Hybrid Assays

Work published by others has already demonstrated that ILK can behave as an adaptor protein as well as a

kinase [19, 20, 22]. Besides integrin, ILK can bind paxillin, PINCH, and actopaxin/CHILKBP/affixin, all components of adhesion complexes [21, 25–27]. We have discovered through yeast two-hybrid assays that ILK can also bind UNC-112, a recently described member of the ERM family of proteins that localizes to myofilament adhesion complexes in nematode body-wall muscle [11]. Using UNC-112 as the bait protein in a yeast two-hybrid screen of a *C. elegans* cDNA library, we identified several positive clones encoding PAT-4/ILK.

Full-length UNC-112 and full-length PAT-4/ILK interact strongly in the yeast two-hybrid system (Figures 7A and 7B). To map the regions of UNC-112 and PAT-4/ILK that are required for this interaction, we made a series of in-frame deletions and found that the amino half of UNC-112, corresponding to amino acid residues 1–396, is critical for its ability to bind PAT-4/ILK, as demonstrated by the significant decrease in the number of viable yeast colonies when these residues are removed from UNC-112 (Figure 7A). Residues 213–474 of PAT-4/ILK, corresponding to the carboxy-terminal kinase domain, were found to be required for PAT-4/ILK to bind full-length UNC-112 (Figure 7B). This is the same region identified as binding actopaxin [28]. Results from in vitro binding assays performed with purified recombinant UNC-112 and PAT-4 are consistent with direct binding between UNC-112 and PAT-4/ILK (Figure 7C). PINCH binds to the amino ankyrin repeats of ILK [21], and we observe that UNC-97/PINCH and PAT-4/ILK interact in an analogous manner (Figure 7D). In addition, using UNC-97/PINCH as the bait protein in a yeast two-hybrid screen of a *C. elegans* library, we identified positive clones containing PAT-4/ILK. One surprise from the *Drosophila* study of ILK was that no detectable interaction was found between dILK and the COOH tail of β PS integrin [23]. We also fail to detect an interaction between PAT-4/ILK and the β PAT-3 integrin cytoplasmic domain in a yeast two-hybrid assay (Figure 7D).

Previous work has shown that a point mutation in human ILK corresponding to E359K confers dominant-negative activity to ILK, presumably by disrupting ILK catalytic activity [22]. However, when the equivalent mutation was introduced into *Drosophila* ILK, it did not

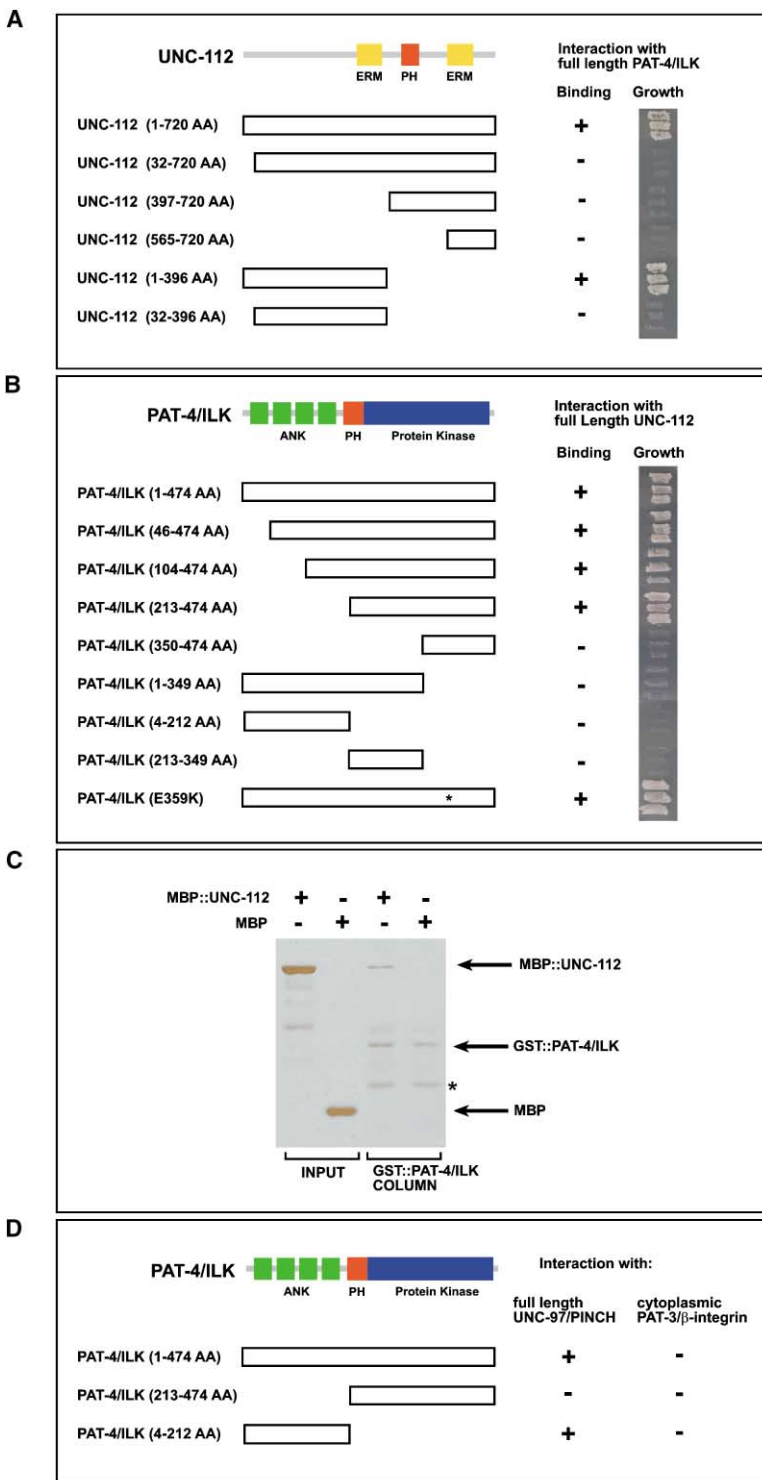


Figure 7. Yeast Two-Hybrid Analysis of UNC-112 and PAT-4/ILK Interactions

The plus and minus symbols provide an indication of how well the yeast grew, and the strip on the right shows three replicate yeast clones grown on selective media.

(A) Interactions between various regions of UNC-112 (open boxes) and full-length PAT-4.

(B) Interactions between various regions of the PAT-4 protein (open boxes) and full-length UNC-112.

(C) We tested the ability of either a fusion between UNC-112 and maltose binding protein (MBP), or MBP alone, to bind to purified GST::PAT-4/ILK in vitro. As shown in Figure 6C, MBP::UNC-112 binds to GST::PAT-4/ILK (lane 3), but MBP alone fails to bind to GST::PAT-4/ILK (lane 4). Degradation products of GST::PAT-4/ILK are indicated by an asterisk. MBP::UNC-112 fails to bind GST only (data not shown).

(D) Interactions between various regions of PAT-4/ILK (open boxes) and full-length UNC-97/PINCH or the cytoplasmic domain of βPAT-3 integrin.

disrupt the in vivo function of this protein, and it rescued the mutant phenotype [23], suggesting that dILK can function independently of its kinase activity. We were interested to see if disruption of the kinase would inhibit protein-protein interactions in the two-hybrid assay. When we introduced the equivalent mutation into PAT-4/ILK, we noticed no decrease in PAT-4/ILK's ability to bind UNC-112 (Figure 7B). This result reinforces the

observations made in *Drosophila* and suggests that PAT-4/ILK is primarily acting as an adaptor molecule at this stage in development.

PAT-4 Functions as an Adaptor during Attachment Assembly

The accumulating evidence that ILK is an adaptor molecule within adhesion complexes and the striking obser-

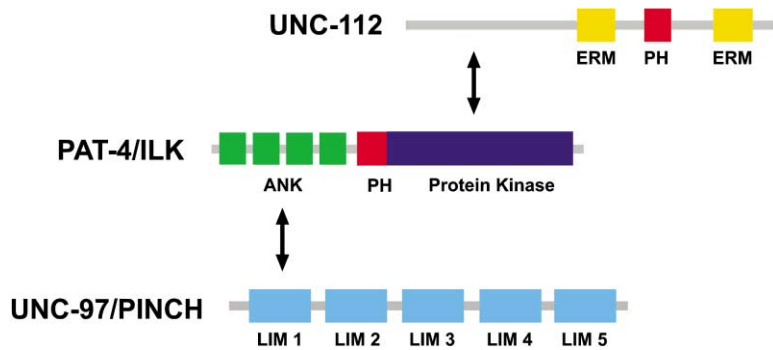


Figure 8. Summary of Interactions between PAT-4/ILK, UNC-112, and UNC-97/PINCH

The carboxy kinase domain of wild-type and kinase-dead PAT-4/ILK interacts with the amino-terminal half of UNC-112. PAT-4/ILK interacts with UNC-97/PINCH in a manner analogous to the interaction observed between the vertebrate homologs [21]. Previously, the integrin β_1 subunit cytoplasmic domain, PINCH, actopaxin, CH-ILKBP, affixin, ILKAP, and paxillin [19, 21, 25, 28, 38, 46] have been reported to bind ILK. In this report, we present UNC-112 as a new ILK binding protein.

vation that kinase-dead ILK (E359K) can fully rescue mutant *Drosophila* lacking functional ILK led us to perform a similar experiment. We were able to completely rescue the *pat-4* mutant phenotype when we introduced a *pat-4* transgene containing the E359K mutation into mutant animals. A recent report shows that vertebrate E359K ILK retains approximately 20% of the kinase activity, while the S343A mutant form has no detectable activity [29]. We therefore made a second kinase-dead construct, corresponding to S343A in vertebrate ILK, and this construct also fully rescues the *pat-4* mutant phenotype. Curiously, these animals not only have normal muscle development, but they also appear wild-type in every other respect. This is not the expected result if the kinases were important in other developmental pathways. To further explore this avenue, we examined whether PAT-4/ILK has a role in a Wnt signaling pathway in *C. elegans*.

Biochemical studies have shown that overexpression of ILK in epithelial cells stimulates the β -catenin/LEF signaling pathway, leading to a downregulation in E-cadherin expression and deactivation of GSK-3 β by both direct and PKB/AKT-mediated phosphorylation [20, 22, 24, 30]. In light of these findings, we examined whether PAT-4/ILK plays a role in a Wnt signaling pathway that occurs very early during *C. elegans* development and is responsible for inducing the asymmetric division of the EMS blastomere [31, 32]. In the absence of Wnt signaling and *gsk-3 β* activity, EMS divides to produce two MS-like blastomeres, and embryos produce extra mesodermal tissue. If PAT-4/ILK is indeed required for this signaling process, then we predict that *pat-4* mutant animals should have a mutant phenotype similar to *Wnt* and *gsk-3 β* mutant animals. Our analysis of *pat-4* mutant embryos and the results from our *pat-4(RNAi)* experiments, the latter likely to remove maternally contributed PAT-4/ILK from early embryos [33], are both inconsistent with this predicted outcome. We therefore can provide no evidence that PAT-4/ILK regulates GSK-3 β during Wnt signaling between P2 and EMS.

Discussion

We have shown that the *pat-4* gene encodes the sole ILK homolog in *C. elegans* and that PAT-4/ILK not only colocalizes with integrin at muscle attachments but is essential for proper attachment assembly. During at-

tachment assembly, ILK functions downstream of perlecan and integrin and upstream of vinculin, UNC-89, and the connection of thin and thick filaments to the sarcolemma. Conversely, proper PAT-4/ILK assembly into muscle attachments requires perlecan and integrin, but not vinculin. Interestingly, PAT-4/ILK and UNC-112 exhibit a mutual requirement for their proper recruitment to nascent attachments. The essential function of PAT-4/ILK in *C. elegans* is independent of its kinase activity, consistent with the emerging view that ILK acts primarily as an adaptor protein (Figure 8). Supporting this interpretation, we have identified a binding interaction between PAT-4/ILK and the novel attachment protein UNC-112. Surprisingly, PAT-4/ILK does not bind to the cytoplasmic tail of integrin in yeast two-hybrid assays. This seems peculiar, since it was this interaction with the cytoplasmic tail of integrin that led to the discovery of vertebrate ILK [19], and yet a result similar to ours was recently reported for *Drosophila* ILK and integrin [23].

The colocalization of PAT-4/ILK with integrin in *C. elegans* muscle attachments is consistent with the previously reported colocalization of ILK and integrin in vertebrate focal adhesions [24] and within *Drosophila* muscle attachments [23]. Our analysis of *pat-4* mutants provides direct evidence that ILK is needed for the proper assembly of muscle attachments. Early events during assembly, including the deposition of UNC-52/perlecan and the initial polarization and clustering of integrin into foci, occur normally. Subsequent events, including the patterning of the foci within the plane of the membrane and the linkage of myofilaments to the nascent attachments, do not occur. This is shown by the failure of integrin foci to enter into the highly ordered array that is characteristic of dense bodies and M-lines, the compromised recruitment of vinculin and UNC-89 to dense bodies and M-lines, respectively, and the failure of actin and myosin filaments to associate normally with the sarcolemma [15]. Mutations removing several other attachment or sarcomere proteins do not cause dramatic deficits in integrin patterning within the plane of the membrane. Specifically, integrin organizes into recognizable arrays of dense bodies and M-lines in the absence of vinculin or myosin A, despite the fact that sarcomere assembly is severely disrupted in either case [4]. Together, these results indicate that a key set of proteins including PAT-4/ILK and UNC-112 pattern the nascent attachments within the plane of the membrane. Other attachment and sarcomere proteins are subse-

quently recruited, but they do not play an essential role in setting up the initial pattern.

Our observations that PAT-4/ILK fails to properly organize in the absence of perlecan or integrin were predicted because perlecan and integrin are required to form nascent dense bodies and M-lines [15, 34]. The failure of PAT-4/ILK to assemble at the membrane in the absence of integrin directly contrasts the results in *Drosophila* in which dILK localizes to muscle attachment sites in integrin mutants [23]. There is also a significant difference between *Drosophila* and *C. elegans* regarding the effects of ILK loss-of-function mutations on muscle attachment assembly [23]. In *Drosophila*, loss of ILK compromises the stability of attachments but does not cause an obvious defect in their initial formation or in the assembly of sarcomeres. This is in marked contrast to the severe effects on attachment and sarcomere assembly that we observe in *pat-4* mutants. Interestingly, assembly defects observed in the muscle of ILK mutants in *Drosophila* and *C. elegans* mirror those seen in integrin loss-of-function mutants in these organisms [35–37]. It is noteworthy that *Drosophila* muscle attachments lacking integrin are able to form while *C. elegans* integrin mutants never form attachments, suggesting that there may be fundamental differences in integrin's role during muscle development in these two organisms.

The comparable rescue of *pat-4* mutants by wild-type and several different kinase-dead *pat-4* transgenes shows that the essential function of ILK is not dependent upon its kinase activity. Experiments using kinase-dead forms of the protein and investigation of early embryonic Wnt signaling pathways both failed to provide any evidence that ILK functions as a kinase during signal transduction. Taken together, our results are consistent with the idea originally proposed by Zervas [23] that the ILK kinase domain is “vestigial”, working as a binding site rather than as a physiologically relevant kinase. The proposed role for vertebrate ILK in integrin signaling may reflect a newly acquired function for this protein. Alternatively, the effects on cellular signal transduction that have been observed in vertebrate cells might be due to nonspecific promiscuous kinase activity caused by ectopic overexpression. Conservation of the ILK kinase domain across species may reflect a conserved structural motif required for its interaction with various pairing partners, including UNC-97/PINCH, UNC-112, and actopaxin/CHILKBP/affixin.

It is important to note, however, that our results do not rule out a role for ILK in signal transduction, since other kinases with overlapping function may compensate for the ILK loss-of-function or kinase-dead mutations that we used in our experiments. We also may have failed to identify subtle developmental deficits that might yet provide evidence that PAT-4/ILK is involved in signal transduction. Nevertheless, our rescue results are remarkably similar to the kinase-dead rescue of *Drosophila* ILK mutants.

If ILK is not a signaling kinase, which is what our experiments and those on *Drosophila* ILK suggest, then its role in adhesion complexes is most likely as an adaptor protein bringing other components of the complex together. The recent identification of additional binding partners of ILK reinforces this conclusion [21, 25, 27,

28, 38]. Using the yeast two-hybrid approach, we have reproduced the binding of ILK and PINCH homologs in *C. elegans*. We have also identified a novel ILK binding partner, the dense body and M-line protein UNC-112. Several lines of evidence are consistent with a direct binding interaction between PAT-4/ILK and UNC-112. First, PAT-4/ILK and UNC-112 colocalize in vivo at dense body and M-line muscle attachments. Second, we have shown that PAT-4/ILK and UNC-112 are reciprocally dependent upon each other for recruitment to the sarcolemma, raising the interesting possibility that they may be recruited to nascent attachments as part of a multi-protein complex. Third, we have identified the subdomains of PAT-4/ILK and UNC-112 that are necessary and sufficient for interaction in yeast two-hybrid assays. Finally, we have obtained evidence for direct binding between purified recombinant PAT-4/ILK and UNC-112 in vitro.

Conclusions

In conclusion, PAT-4/ILK mediates the formation of linkages between the nascent adhesion complexes and the underlying cytoskeleton. Failure to complete these linkages in the absence of PAT-4/ILK blocks sarcomere assembly, paralyzes the embryo, and ultimately results in developmental arrest. On the cellular level, the nascent muscle attachments remain disorganized within the plasma membrane. PAT-4/ILK function in vivo appears to be independent of its kinase activity. Our results suggest that PAT-4/ILK is an adaptor protein. Consistent with this view, we have identified a new ILK binding partner, the novel protein UNC-112.

Experimental Procedures

Strains and Genetics Used in This Study

Worms were grown and genetic analysis was done as described [39]. Wild-type worms are the N2 strain of the Bristol variety. The following mutations and strains were used: *deb-1(st555)*, *pat-2(st567)*, *pat-3(st552)*, *pat-4(st551)*, *pat-4(st559)*, *pat-4(st579)*, *pat-4(st580)*, *unc-52(st549)*, *unc-112(gk-1)*, *unc-112(st561)*, WB72 (*pat-4(st551); zEx55*), WB125 (*pat-4(st551); zEx194*), WB154 (*unc-44(e362) deb-1(st555)/unc-82(e1223) unc-24(e138); zEx194*), WB156 (+/+; *zEx194*), WB175 (*pat-4(st551); zEx209*), WB201 (*pat-4(st551); zEx204*), and WB204 (*pat-4(st551); zEx225*). All extrachromosomal arrays contain the dominant transformation marker pRF4 (*rol-6*) and the following: *zEx55* contains a PCR fragment, generated using primers BW48/BW48 (all primer sequences are available in Table S1 of the Supplementary Material available with this article online, see below), corresponding to full-length *pat-4*; *zEx194* contains plasmid pAT4.4; *zEx204* contains PCR fragments (generated using primers T7/BW15, BW163/2051, BW70/2051, and BW71/BW94), corresponding to *pat-3::CFP* and *pat-4::YFP*; *zEx209* contains plasmid pAT4.6; and *zEx225* contains plasmids pAT4.21. The molecular lesions corresponding to *pat-4* alleles *st551*, *st559*, *st579*, and *st580* were identified by PCR amplification of the C29F9.7 gene from homozygous *Pat* embryos and subsequent DNA sequencing using the *fmoI* kit (Promega). We used PCR to define the right breakpoints of the *st559* and *st580* deletion alleles to an interval defined by the *pat-4* locus and *K10F12.3*, which is located 230 kbp to the right. The left breakpoints were defined using PCR primers corresponding to the 5' region of the predicted gene *F54C4.3*, which is located 3.2 kbp to the left of *pat-4*. We are able to detect the PCR product using *pat-4(st580)* embryos as templates, but not when we use *pat-4(st559)* embryos as templates. cDNA clone yk199a2 was sequenced and found to be a full-length *pat-4* clone whose sequence matches the processed transcript predicted by GENEFINDER. Seven additional full-length cDNA clones from Yuji

Kohara's cDNA collection (yk175b10, yk269g8, yk334c3, yk374e3, yk415h4, yk445c5, and yk473d6) were also analyzed, and no alternatively spliced isoforms were detected. The *pat-4* nucleotide and protein sequence have been previously submitted to GenBank/EMBL/DDBJ under the accession number T33574 [40]. PAT-4 homologs were identified using the BLAST algorithm to search the NCBI database, and sequence alignments were performed using the CLUSTAL V alignment method. Transformation rescue of *pat-4(st551)* was done by injecting cosmid DE10 (canonical for C29F9) [41]. To confirm that *pat-4* corresponds to C29F9.7, we injected *pat-4(st551)/+* animals with a PCR product corresponding only to C29F9.7. The promoter sequence used for this PCR product starts 1915 bp upstream from the predicted ATG start codon. Both injection mixes completely rescue the *pat-4* phenotype.

Molecular Biology

Plasmids pAT4.4, pAT4.6, pAT4.16, and pAT4.21 are *pat-4::gfp* minigenes in which the *pat-4*-coding region is fused in frame to the carboxy terminus of GFP. These minigenes either contain no *pat-4* intronic sequence (pAT4.16) or contain the first intron of *pat-4* (pAT4.4, pAT4.6, and pAT4.21). Plasmid pAT4.1 was constructed by cloning a PCR fragment, generated using primers BW73 and BW59, into the 4285-bp BamHI-NcoI fragment of plasmid yk199a2 (GenBank accession number C39322). This plasmid contains 1915 bp of 5' UTR sequence and the first intron of the *pat-4* gene. The plasmid pAT4.3 was constructed by cloning a PCR product, generated using primers BW99 and BW100 and corresponding to full-length *pat-4* cDNA, into the vector pPD118.20 digested with EcoRI. The 2.13-kb MluI-KpnI fragment of the resulting plasmid was then replaced with a PCR product generated using BW-116 and BW-118 and digested with MluI and KpnI. The plasmid pAT4.4 was constructed by replacing the 235-bp BstXI-EagI fragment of pAT4.3 with the 783-bp BstXI-EagI fragment of pAT4.1. A mutagenic PCR fragment, generated with primers BW190 and BW191 and corresponding to vertebrate kinase-dead (E359K) ILK, was cloned into the 6.69-kb SacI-NheI fragment of either pAT4.4 or pAT4.3 to generate pAT4.6 or pAT4.16, respectively. The plasmid pAT4.21 was constructed by replacing the 368-bp SacI-NheI wild-type-coding sequence of pAT4.4 with a mutagenic PCR fragment generated with primers BW229 and BW230, corresponding to vertebrate kinase-dead (S343A) ILK. All plasmids were verified by sequencing.

A cDNA fragment of *unc-112* was PCR amplified using primers Bam-unc-112 and unc-112-NsiXho. This fragment was cloned into pBluescript KS+ to make pDM#224. The NsiI-XhoI region of pDM#224 was exchanged for the NsiI-XhoI region of pDM#205, a cDNA clone of *unc-112*, see [11], to make pDM#225. A BamHI-XhoI fragment of pDM#225 was cloned into the BamHI-SalI sites of pGBDU-C1 or pGAD-C1, resulting in pDM#235 or pDM#236, respectively (amino acids [aa] 1–720). pDM#238 was made by inserting the BamHI-BglII fragment of pDM#225 into pGAD-C1. To make pDM#230 (aa 397–720), a BglII-XhoI fragment of pDM#205 was inserted into pGAD-C3. pDM#232 (aa 565–720) and pDM#234 (aa 32–720) were made by cloning a SnaBI (blunt ended with Klenow fragment) and XhoI, or a Styl (blunt ended with Klenow fragment) and XhoI fragment, of pDM#205 into the SmaI and XhoI sites of pGAD-C1. pDM#264 (aa 32–396) was made by removing the BglII-XhoI region from pDM#234.

Among the *pat-4* deletion plasmids, pDM#280, pDM#312, and pDM#313 were originally isolated by two-hybrid screening with the UNC-112 bait. To make the full-length PAT-4 plasmid pDM#292 (aa 1–474), the XhoI fragment of pDM#280 was inserted into the Sall site of pGBDU-C2. pDM#301 (aa 213–349), pDM#327 (aa 4–212), and pDM#328 were made by inserting Sall-Sall or Sall-BglII fragments of pDM#292 into Sall sites of pGBDU-C1, pGBDU-C3, or pGAD-C3. pDM#303 (aa 350–474) and pDM#304 were made by inserting a Sall-BglII fragment of pDM#292 into Sall-BglII sites of pGBDU-C1 and pGAD-C1. To make pDM#325 (aa 213–474) and pDM#326, a Sall-Sall fragment of pDM#302 was cloned into a Sall site of pDM#303 or pDM#304. pDM#323 (aa 1–349) was made by exchanging an EcoRI-SacII region of pDM#301 for that of pDM#292. The EcoRI-SmaI fragment of pAT4.16.2 was cloned into the EcoRI and SmaI sites of pDM#303 to make pDM#381 (E359K). pDM#321 (aa 46–474) and pDM#322 (aa 104–474) were made by cloning an XhoI fragment of pDM#312 and pDM#313 into the Sall site of pGBDU-C2.

A cDNA fragment of the *pat-3* cytoplasmic region was PCR amplified using primers Bam-pat-3cyto and pat-3cyto-Xho. This fragment was cloned into pBluescript KS+ to make pDM#226. The BamHI-XhoI fragment of pDM#226 was cloned into pGBDU-C1 to make pDM#227. A cDNA fragment of *unc-97* was PCR amplified using primers pU97-1 and pU97-2. This fragment was digested with BamHI and XhoI and was subsequently cloned into the BamHI and Sall sites of pGBDU-C1 to make pDM#429.

A plasmid for bacterial expression of GST::PAT-4 (C terminus, aa 213–474) fusion (pDM#438) was made by inserting a BamHI-BglII fragment of pDM#325 into pGEX-KK-1 (a gift from Dr. Kaibuchi). To make pDM#367 for bacterial expression of the MBP::UNC-112 (N terminus, aa 1–396) fusion, a BamHI-BglII fragment of pDM#225 was cloned into pMAL-KK-1 (a gift from Dr. Kaibuchi).

RNAi was performed according to [33]. dsRNA corresponding to *pat-4* was generated using the MegaScribe kit (Ambion) and the cDNA clone yk199a2 as a template.

In Vitro Binding Assay

GST::PAT-4 and MBP::UNC-112 were prepared from *E. coli* harboring pDM#438 and pDM#367, respectively, and the interaction of GST::PAT-4 with MBP::UNC-112 was examined as described [42]. Briefly, MBP alone or MBP::UNC-112 (25 μ g) were mixed with glutathione affinity beads coated with GST::PAT-4 (10 μ g). The beads were then washed with buffer containing 100 mM NaCl and 0.1% Triton X-100, and the bound proteins were extracted by the addition of SDS-PAGE sample buffer. The extracts were subjected to SDS-PAGE, followed by silver staining.

Antibody Staining

Populations of embryos were fixed and stained as previously described [16]. We used affinity-purified goat anti-mouse IgG conjugated to rhodamine (Chemicon International) diluted 1:100 as the secondary antibody. For our analysis, we used the following monoclonal antibodies, diluted in PBS supplemented with 0.5% Tween-20 and 30% normal goat serum: MH2 (1:100), MH24 (1:200), MH25 (1:250), MH27 (1:1500), and MH42 (1:50) [12, 43]. Polyclonal PAT-4 antisera was obtained from mice injected with a synthetic 31 amino acid peptide (CKNTILEIAQEHGQSPNDRVFPKDTTWKGTK; single letter amino acid notation).

Two-Hybrid Screening

Two-hybrid screening with the UNC-112 bait was performed using the yeast strain PJ69-4A harboring pDM#235 as described [44]. Yeast cells were transformed by the lithium acetate method [45]. After transformation with the RB2 cDNA library (a gift from Dr. R. Barstead), His⁺ colonies were selected. HIS3 expression was assayed using 2 mM 3-amino triazole. Two-hybrid interaction was confirmed by ADE2 expression. Isolated library plasmids were confirmed. PCR-amplified cDNA fragments of library plasmids were subjected to DNA sequencing. From 5×10^6 colonies, *pat-4* cDNA clones pDM#280, pDM#312, and pDM#313 were identified. To confirm two-hybrid interactions, three independent colonies were selected and assayed for colony formation.

Supplementary Material

Supplementary Material including Table S1, which lists primer sequences, is available at <http://images.cellpress.com/supmat/supmatin.htm>.

Acknowledgments

We are grateful to Dr. Andy Fire and his lab for plasmid vectors, Dr. Alan Coulson for cosmids, Dr. Yuji Kohara for cDNA clones, Dr. Robert Barstead for the RB2 cDNA library, Dr. Kozo Kaibuchi for plasmids, Dr. Shinya Kuroda for advice on in vitro binding assays, and Dr. John Speith and the *C. elegans* Genome Sequencing Consortium for *pat-4* DNA sequence data. We wish to thank the lab of Akira Chiba for allowing us the use of equipment and reagents. We appreciate the technical assistance provided by Chris Zugates and Patrick King. Some of the nematode strains used in this work were provided by the *Caenorhabditis* Genetics Center, which is funded by the National Institutes of Health National Center for Research

Resources (NCRR). This work was supported by a predoctoral fellowship from the American Heart Association, Midwest Affiliate to A.C.M.; a Japan Society for the Promotion of Science Postdoctoral Fellowship for Research Abroad (2000) to H.Q.; a grant from the Canadian Institute for Health Research to D.G.M.; and National Institutes of Health grant R01 HD38464-01 and a Scientist Development Grant from the American Heart Association, Midwest Affiliate to B.D.W.

Received: January 17, 2002

Revised: March 4, 2002

Accepted: March 7, 2002

Published: May 14, 2002

References

1. Moerman, D.G., and Fire, A. (1997). Muscle: Structure, function, and development. In *C. elegans* II. D.L. Riddle, T. Blumenthal, B.J. Meyer, and J.R. Priess, eds. (Cold Spring Harbor, NY: Cold Spring Harbor Laboratory Press), pp. 417–470.
2. Waterston, R.H. (1988). Muscle. In *The Nematode Caenorhabditis elegans*. W.B. Wood, ed. (Cold Spring Harbor, NY: Cold Spring Harbor Press), pp. 281–335.
3. Epstein, H.F., Casey, D.L., and Ortiz, I. (1993). Myosin and paramyosin of *Caenorhabditis elegans* embryos assemble into nascent structures distinct from thick filaments and multi-filament assemblages. *J. Cell Biol.* 122, 845–858.
4. Hresko, M.C., Williams, B.D., and Waterston, R.H. (1994). Assembly of body wall muscle and muscle cell attachment structures in *Caenorhabditis elegans*. *J. Cell Biol.* 124, 491–506.
5. Schnabel, R., Hutter, H., Moerman, D., and Schnabel, H. (1997). Assessing normal embryogenesis in *Caenorhabditis elegans* using a 4D microscope: variability of development and regional specification. *Dev. Biol.* 184, 234–265.
6. Sulston, J.E., Schierenberg, E., White, J.G., and Thomson, J.N. (1983). The embryonic cell lineage of the nematode *Caenorhabditis elegans*. *Dev. Biol.* 100, 64–119.
7. Rogalski, T.M., Williams, B.D., Mullen, G.P., and Moerman, D.G. (1993). Products of the *unc-52* gene in *Caenorhabditis elegans* are homologous to the core protein of the mammalian basement membrane heparan sulfate proteoglycan. *Genes Dev.* 7, 1471–1484.
8. Gettner, S.N., Kenyon, C., and Reichardt, L.F. (1995). Characterization of β PAT-3 heterodimers, a family of essential integrin receptors in *C. elegans*. *J. Cell Biol.* 129, 1127–1141.
9. Moulder, G.L., Huang, M.M., Waterston, R.H., and Barstead, R.J. (1996). Talin requires β -integrin, but not vinculin, for its assembly into focal adhesion-like structures in the nematode *Caenorhabditis elegans*. *Mol. Biol. Cell* 7, 1181–1193.
10. Hobert, O., Moerman, D.G., Clark, K.A., Beckerle, M.C., and Ruvkun, G. (1999). A conserved LIM protein that affects muscular adherens junction integrity and mechanosensory function in *Caenorhabditis elegans*. *J. Cell Biol.* 144, 45–57.
11. Rogalski, T.M., Mullen, G.P., Gilbert, M.M., Williams, B.D., and Moerman, D.G. (2000). The *unc-112* gene in *Caenorhabditis elegans* encodes a novel component of cell-matrix adhesion structures required for integrin localization in the muscle cell membrane. *J. Cell Biol.* 150, 253–264.
12. Francis, G.R., and Waterston, R.H. (1985). Muscle organization in *Caenorhabditis elegans*: localization of proteins implicated in thin filament attachment and I-band organization. *J. Cell Biol.* 101, 1532–1549.
13. Barstead, R.J., and Waterston, R.H. (1989). The basal component of the nematode dense-body is vinculin. *J. Biol. Chem.* 264, 10177–10185.
14. Benian, G.M., Tinley, T.L., Tang, X., and Borodovsky, M. (1996). The *Caenorhabditis elegans* gene *unc-89*, required for muscle M-line assembly, encodes a giant modular protein composed of Ig and signal transduction domains. *J. Cell Biol.* 132, 835–848.
15. Williams, B.D., and Waterston, R.H. (1994). Genes critical for muscle development and function in *Caenorhabditis elegans* identified through lethal mutations. *J. Cell Biol.* 124, 475–490.
16. Barstead, R.J., and Waterston, R.H. (1991). Vinculin is essential for muscle function in the nematode. *J. Cell Biol.* 114, 715–724.
17. Dedhar, S. (2000). Cell-substrate interactions and signaling through ILK. *Curr. Opin. Cell Biol.* 12, 250–256.
18. Dedhar, S., Williams, B., and Hannigan, G. (1999). Integrin-linked kinase (ILK): a regulator of integrin and growth-factor signalling. *Trends Cell Biol.* 9, 319–323.
19. Hannigan, G.E., Leung-Hageteijn, C., Fitz-Gibbon, L., Coppolino, M.G., Radeva, G., Filmus, J., Bell, J.C., and Dedhar, S. (1996). Regulation of cell adhesion and anchorage-dependent growth by a new β_1 -integrin-linked protein kinase. *Nature* 379, 91–96.
20. Delcommenne, M., Tan, C., Gray, V., Rue, L., Woodgett, J., and Dedhar, S. (1998). Phosphoinositide-3-OH kinase-dependent regulation of glycogen synthase kinase 3 and protein kinase B/AKT by the integrin-linked kinase. *Proc. Natl. Acad. Sci. USA* 95, 11211–11216.
21. Tu, Y., Li, F., Goicoechea, S., and Wu, C. (1999). The LIM-only protein PINCH directly interacts with integrin-linked kinase and is recruited to integrin-rich sites in spreading cells. *Mol. Cell Biol.* 19, 2425–2434.
22. Novak, A., Hsu, S.C., Leung-Hageteijn, C., Radeva, G., Papkoff, J., Montesano, R., Roskelley, C., Grosschedl, R., and Dedhar, S. (1998). Cell adhesion and the integrin-linked kinase regulate the LEF-1 and β -catenin signaling pathways. *Proc. Natl. Acad. Sci. USA* 95, 4374–4379.
23. Zervas, C.G., Gregory, S.L., and Brown, N.H. (2001). *Drosophila* integrin-linked kinase is required at sites of integrin adhesion to link the cytoskeleton to the plasma membrane. *J. Cell Biol.* 152, 1007–1018.
24. Wu, C., Keightley, S.Y., Leung-Hageteijn, C., Radeva, G., Coppolino, M., Goicoechea, S., McDonald, J.A., and Dedhar, S. (1998). Integrin-linked protein kinase regulates fibronectin matrix assembly, E-cadherin expression, and tumorigenicity. *J. Biol. Chem.* 273, 528–536.
25. Nikolopoulos, S.N., and Turner, C.E. (2001). Integrin-linked kinase (ILK) binding to paxillin LD1 motif regulates ILK localization to focal adhesions. *J. Biol. Chem.* 276, 23499–23505.
26. Nikolopoulos, S.N., and Turner, C.E. (2000). Actopaxin, a new focal adhesion protein that binds paxillin LD motifs and actin and regulates cell adhesion. *J. Cell Biol.* 151, 1435–1448.
27. Wu, C. (1999). Integrin-linked kinase and PINCH: partners in regulation of cell-extracellular matrix interaction and signal transduction. *J. Cell Sci.* 112, 4485–4489.
28. Tu, Y., Zhang, Y., Hua, Y., and Wu, C. (2001). A new focal adhesion protein that interacts with integrin-linked kinase and regulates cell adhesion and spreading. *J. Cell Biol.* 153, 585–598.
29. Persad, S., Attwell, S., Gray, V., Mawji, N., Deng, J.T., Leung, D., Yan, J., Sanghera, J., Walsh, M.P., and Dedhar, S. (2001). Regulation of protein kinase B/Akt-serine 473 phosphorylation by integrin-linked kinase: critical roles for kinase activity and amino acids arginine 211 and serine 343. *J. Biol. Chem.* 276, 27462–27469.
30. Dedhar, S. (1999). Integrins and signal transduction. *Curr. Opin. Hematol.* 6, 37–43.
31. Rocheleau, C.E., Downs, W.D., Lin, R., Wittmann, C., Bei, Y., Cha, Y.H., Ali, M., Priess, J.R., and Mello, C.C. (1997). Wnt signaling and an APC-related gene specify endoderm in early *C. elegans* embryos. *Cell* 90, 707–716.
32. Thorpe, C.J., Schlesinger, A., Carter, J.C., and Bowerman, B. (1997). Wnt signaling polarizes an early *C. elegans* blastomere to distinguish endoderm from mesoderm. *Cell* 90, 695–705.
33. Fire, A., Xu, S., Montgomery, M.K., Kostas, S.A., Driver, S.E., and Mello, C.C. (1998). Potent and specific genetic interference by double-stranded RNA in *Caenorhabditis elegans*. *Nature* 391, 806–811.
34. Rogalski, T.M., Gilchrist, E.J., Mullen, G.P., and Moerman, D.G. (1995). Mutations in the *unc-52* gene responsible for body wall muscle defects in adult *Caenorhabditis elegans* are located in alternatively spliced exons. *Genetics* 139, 159–169.
35. Brown, N.H. (1994). Null mutations in the α PS2 and β PS integrin subunit genes have distinct phenotypes. *Development* 120, 1221–1231.
36. Zusman, S., Grinblat, Y., Yee, G., Kafatos, F.C., and Hynes,

- R.O. (1993). Analyses of PS integrin functions during *Drosophila* development. *Development* **118**, 737–750.
37. Volk, T., Fessler, L.I., and Fessler, J.H. (1990). A role for integrin in the formation of sarcomeric cytoarchitecture. *Cell* **63**, 525–536.
 38. Yamaji, S., Suzuki, A., Sugiyama, Y., Koide, Y., Yoshida, M., Kanamori, H., Mohri, H., Ohno, S., and Ishigatsubo, Y. (2001). A novel integrin-linked kinase-binding protein, affixin, is involved in the early stage of cell-substrate interaction. *J. Cell Biol.* **153**, 1251–1264.
 39. Brenner, S. (1974). The genetics of *Caenorhabditis elegans*. *Genetics* **77**, 71–94.
 40. The *Caenorhabditis elegans* Sequencing Consortium. (1998). Genome sequence of the nematode *C. elegans*: a platform for investigating biology. *Science* **282**, 2012–2018.
 41. Mello, C., and Fire, A. (1995). DNA transformation. *Methods Cell Biol.* **48**, 451–482.
 42. Kuroda, S., Fukata, M., Nakagawa, M., Fujii, K., Nakamura, T., Ookubo, T., Izawa, I., Nagase, T., Nomura, N., Tani, H., et al. (1998). Role of IQGAP1, a target of the small GTPases Cdc42 and Rac1, in regulation of E-cadherin-mediated cell-cell adhesion. *Science* **281**, 832–835.
 43. Francis, R., and Waterston, R.H. (1991). Muscle cell attachment in *Caenorhabditis elegans*. *J. Cell Biol.* **114**, 465–479.
 44. James, P., Halladay, J., and Craig, E.A. (1996). Genomic libraries and a host strain designed for highly efficient two-hybrid selection in yeast. *Genetics* **144**, 1425–1436.
 45. Ito, H., Fukuda, Y., Murata, K., and Kimura, A. (1983). Transformation of intact yeast cells treated with alkali cations. *J. Bacteriol.* **153**, 163–168.
 46. Leung-Hageteijn, C., Mahendra, A., Naruszewicz, I., and Hannigan, G.E. (2001). Modulation of integrin signal transduction by ILKAP, a protein phosphatase 2C associating with the integrin-linked kinase, ILK1. *EMBO J.* **20**, 2160–2170.